The Effect of Activated flux and shielding gas mix of Argon-Nitrogen on the bead geometry of Duplex Stainless Steel 2205 Gas Tungsten Arc Welds

R. Sasidharan, S.R. Koteswara Rao, S.Vijayan

Gas Tungsten Arc Welding (GTAW) is widely used to fabricate duplex stainless-steel structures. While the process offers clean welds, it is difficult to achieve full penetration in flat butt joints thicker than 3mm, that are common in pipe welds. This study aims at obtaining single pass full penetration welds in 6 mm thick plates with flat butt joint configuration, which can avoid use of filler material and minimize edge preparation. Use of activated flux and addition of nitrogen to the shielding gas have been employed to obtain single pass full penetration autogenous welds on 6mm thick plates. The effect of welding current, welding speed, arc gap and gas flow rate have been studied while using Activated flux and nitrogen addition.

In this investigation the effect of shielding gas argon and argon plus nitrogen are studied on the bead geometry of Activated flux assisted GTA welds of Duplex Stainless Steel 2205, 6 mm thick plates. The ATIG process parameters were optimized using Taguchi L16 orthogonal array. Current (A), Welding Speed (mm/min), Gas Flow Rate (L/min) and Arc Gap (mm) are the input process parameters considered while the depth of penetration is the response to be maximized. It has been concluded that the welding speed and current are the dominant parameters affecting the response with and without the inclusion of nitrogen in the shielding gas respectively. Nitrogen addition seemingly reduced the depth of penetration.

KEYWORDS: DUPLEX STAINLESS STEEL (2205), ACTIVATED FLUX GTA WELDING, TAGUCHI L16 OPTIMIZATION, BEAD GEOMETRY

INTRODUCTION

A novel variation of the TIG welding procedure known as the Activated flux ATIG welding technique was initially created for the welding of titanium by Paton Institute of Electric Welding to boost penetration capability by up to 200% when compared with conventional welding. TIG welding makes use of a non-consumable tungsten electrode to form the weld. To prevent oxidation and contamination, the arc is shielded by an inert gas such as argon or helium.

ATIG welding is like TIG welding, except it adds an extra gas, usually nitrogen, to the welding arc. This active gas increases weld penetration and improves the mechanical qualities of the weld joint. In ATIG process, just prior to welding, an active flux is applied and deposited on the workpiece surface by brushing or spraying the flux layers onto the workpiece's surface. Welding happens when the surface has been dried and layer deposition is finished. The flux helps in arc striking and arc stability.

R.Sasidharan
Department of Mechanical Engineering,
Tagore Engineering College, Chennai, India

S.R. Koteswara Rao, S.Vijayan
Department of Mechanical Engineering,
Sri Sivasubramaniya Nadar College of Engineering, Chennai, India

The slag produced will shield the weld bead, cover the arc gap, and prevent damage to the molten metal. Deeper penetration is accomplished due to ATIG's improved arc penetrating capabilities. ATIG welding is similar to TIG welding, except it adds an extra gas, usually nitrogen, to the welding arc. This active gas increases weld penetration and improves the mechanical qualities of the weld joint [1]. TIG welding offers precise control and clean welds, but it may not penetrate thicker materials, whereas ATIG welding improves penetration and productivity while enhancing mechanical qualities, albeit at higher cost and complexity. Material thickness, desired weld quality, and available resources all plays a role when choosing what approach should be employed [4 &5].

One of the primary problems with welding duplex stainless steels is the production of weld metals with an excessive quantity of ferrite due to the rapid cooling that takes place during welding. The problem is often resolved by altering the weld metal composition or heat input to obtain the correct phase balance. Nitrogen has a larger heat capacity than other gases, therefore it can absorb and release heat more efficiently. Heat is evenly spread over the workpiece by introducing nitrogen gas flow during the welding process, which prevents localised overheating and minimises distortion [7-10]. This improves control over the perimeters, which leads to precise and appealing welds. The use of nitrogen gas in welding and metal manufacturing can considerably reduce post-weld cleanup time. Nitrogen, being an inert gas, inhibits oxides and scale from forming on the weld surface, minimising the need for considerable cleaning and surface preparation. This saves time and decreases the usage of chemicals and abrasive materials commonly used to remove weld spatter and scale. The cleaner welds achieved with nitrogen gas also make subsequent processes easier, such as painting applications, because they give a smoother and more uniform surface for adhesion [2].The use of duplex stainless steels, which offer excellent resistance to stress corrosion caused by chloride and strong mechanical properties, can help to lessen this problem in pipelines. The metallurgical characteristics of duplex stainless steels, however, pose a variety of technical difficulties during the welding process [21-23]. In welding pipes, the depth of penetration needs to be carefully controlled.

Puren et al analyses the stress corrosion cracking behaviour of 2205 duplex stainless steel welded joints when hydrogen, corrosive media, and stress are combined. The results reveal that the presence of hydrogen causes the fracture to transfer from the base material to the heat affected zone and commence pitting, which leads to crack initiation and stress corrosion fracture [25].The impact of Post Soldering heat treatment (TTPS) parameters 25 s 1050 °C on autogenous TIG welds of UNS S31803 DSS strips, modifies the microstructure which enhances higher corrosion rates observed with higher ferrite content and nitride precipitation [26].The multi-layer multi-pass welding of low-alloy steel and duplex stainless steel, ER2209 welding wire was single-layer single-pass deposited on the surface of Q345B hot-rolled plate using gas metal arc welding (GMAW). The "tongue-shaped" morphology formed due to arc energy and the width of the heat affect zone in the welded joint, affects the corrosion performance of the welded joints [27].

The austenite content in DSS deposits increases with increasing deposition energy, with Ar+2%N2-protected deposits having much greater content than Ar+2%CO2-protected deposits. DSS deposits with balanced phase content (austenite concentration of 48.4%) were achieved at a line energy of 600 J/mm for DED-arc under Ar+2%N2 protection. Unlike the nitrogen loss in Ar+2%CO2-protected samples, Ar+2%N2 shielding gas introduces more nitrogen elements into DSS samples. Ar+2%N2 protected samples contain more austenite and exhibit a more homogenous microstructure, resulting in solid solution strengthening and a significant reduction in the anisotropy of the tensile characteristics [28].Microstructure characterisation of Plasma Arc Welding linked on SDSS 2507 at a thickness of 10 mm characterisation reveals significant changes in austenite content, ranging from 68.9% in weld metal (WM) to 32.1% in the heat-affected zone (HAZ). The oxide inclusions in the WM increase the hardness of the welded joints, but also provide a channel for crack development, reducing its impact toughness. HAZ has a complex microstructure that forms ferrite and a variety of austenite, including grain boundary austenite (GBA), intragrain austenite (IGA), and Widmanstätten austenites (WA). HAZ contains minor amounts of secondary austenite ($\gamma 2$) and chromium nitride, which considerably reduces its corrosion resistance [29]. This paper attempts to optimize the TIG and ATIG welding process's process parameters and their effect on depth of penetration using the Taguchi technique.

EXPERIMENTAL PROCEDURE

Duplex Stainless Steel (2205) plates of 6mm thickness 200X100 mm size are edge prepared to form flat butt joints. The chemical composition of the Duplex Stainless Steel (2205) is listed in the table 1. The joints were autogenously welded using an automatic GTA welding machine. The process parameters considered for study are: Welding Current (A), Welding speed (mm/min), Gas Flow rate (L/min) and Arc gap (mm) [6]. The response variable is Depth of Penetration and width of the weldment. ATIG welding experiments using different shielding gases of Pure argon and mixture of Argon + 2% Nitrogen are carried out by varying the arc gap in the range of 1.8 to 2.4 mm, the gas flow rate in the range of 10–16 litres/min, the welding current in the range of 150–180Amps to and the welding speed in the range of 100–130 mm/min. The process parameters considered are summarized in Table 2. The electrode material and tip angle are kept constant. Taguchi L16 orthogonal design is used for designing the experiments and the experimental layout is shown in Table 3.

Tab. 1 – Chemical Composition of Duplex Stainless Steel Base Metal, weight %

Element	C	Si	Mn	S	P	Cr	Ni	Mo	N
Wt %	0.02	0.33	1.7	0.002	0.02	22.71	5.40	3.02	0.14

Tab. 2 – Activated flux Gas Tungsten Arc welding parameters used to weld 6 mm thick DSS2205 plates

Welding Process Levels(ATIG+N)	Current(A)	Welding speed(mm/min)	Gas flow rate (l/min)	Arc gap (mm)
1	150	100	10	1.8
2	160	110	12	2
3	170	120	14	2.2
4	180	130	16	2.4

Tab. 3 – L16 Orthogonal Array

Experiment No.	Current(A)	Welding speed(mm/min)	Gas flow rate (l/min)	Arc gap (mm)
1	1	1	1	1
2	1	2	2	2
3	1	3	3	3
4	1	4	4	4
5	2	1	2	3
6	2	2	1	4
7	2	3	4	1
8	2	4	3	2
9	3	1	3	4
10	3	2	4	3
11	3	3	1	2
12	3	4	2	1
13	4	1	4	2
14	4	2	3	1
15	4	3	2	4
16	4	4	1	3

Based on the Taguchi design the experiments were conducted and subjected to metallographic observation. Specimens were polished and etched using kalling's reagent No.2 for metallographic observations at mid length of the weld. For each weld, depth of penetration and weld face width were measured using an image analyzer.

RESULT AND DISCUSSION

To the given heat input, the weldments should have maximum penetration and minimal face width, however in case of activated GTA welds, the presence of activated flux changes the temperature gradient to positive value i.e. $d\sigma/dT>0$. This positive temperature gradient presents centripetal marangoni convection which in turn directs the flow toward pool center resulting in deeper and narrow weld pool than the normal TIG welds. In Activated TIG optimization is done to maximize depth of penetration. Depth of penetration falls under higher the better-quality characteristic and the corresponding loss function is expressed by Equation 1. The overall loss function of depth of penetration is further changed into the s/n ratio by Equation 2. In Taguchi method, S/N ratio is used to find out the deviation of the quality characteristics from the preferred value [3,12&24].

$$\mathrm{Lij} = \frac{1}{n}\sum_{1}^{n}\frac{1}{\mathrm{Y_{ij}}^{2}} \tag{1}$$

$$\frac{\mathrm{S}}{\mathrm{N}}\,\mathrm{ratio} = -10\log\left[\mathrm{L_{ij}}\right] \tag{2}$$

The average S/N ratio for all the responses (depth of penetration: DOP) values of all levels are calculated and listed in Table 4.

Tab. 4 – S/N ratio for depth of penetration of Activated TIG Welds.

Experiment No.	ATIG Welds			ATIG+N Welds		
	Width(mm)	Depth D (mm)	S/N ratio for D	Width(mm)	Depth D (mm)	S/N ratio for D
ATIGL1	6.94	4.78	13.59	6.56	4.46	12.98
ATIGL2	7.29	4.56	13.18	7.00	4.45	12.978
ATIGL3	7.34	3.83	11.66	6.50	4.12	12.30
ATIGL4	7.42	3.37	10.55	7.75	3.71	11.38
ATIGL5	7.47	6.12	15.74	7.47	5.79	15.13
ATIGL6	7.72	4.67	13.39	7.25	4.30	12.68
ATIGL7	7.26	4.18	12.42	6.31	3.57	11.058
ATIGL8	7.15	4.37	12.81	6.59	3.85	11.708
ATIGL9	8.33	6.34	16.04	7.34	5.55	14.89
ATIGL10	7.9	5.42	14.68	6.94	4.72	13.47
ATIGL11	7.23	4.48	13.02	7.25	5.09	14.13
ATIGL12	7.05	4.26	12.59	7.31	4.00	12.04
ATIGL13	7.96	6.26	15.93	7.88	6.16	15.79
ATIGL14	7.72	6.31	16.00	7.63	6.09	15.69
ATIGL15	8.28	6.12	15.74	7.25	6.07	15.66
ATIGL16	7.91	4.29	12.65	7.63	4.79	13.60

STATISTICAL ANALYSIS

Analysis of variance (ANOVA) is performed on the S/N ratio using a commercially available software package for both ATIG and ATIG+N based results. The results are provided in Tables 5& 6.

Tab. 5 – Analysis of Variance for ATIG - DEPTH of penetration (mm)

Source	DoF	Seq SS	Adj SS	Adj MS	F	P	% of contribution
Current	3	5.36	5.36	1.79	11.85	0.036	36.88
Welding Speed	3	7.19	7.19	2.40	15.90	0.024	49.50
Gas Flow Rate	3	1.38	1.38	0.46	3.04	0.193	9.47
Arc Gap	3	0.15	0.15	0.05	0.33	0.808	1.02
Error	3	0.45	0.45	0.15			3.11
Total	15	14.53					100

R-Sq = 96.89%   R-Sq(adj) = 84.43%

Tab. 6 – Analysis of Variance for ATIG+N - DEPTH of penetration (mm)

Source	DoF	Seq SS	Adj SS	Adj MS	F	P	% of contribution
Current	3	19.16	19.16	6.39	8.48	0.056	50.16
Welding Speed	3	12.99	12.99	4.33	5.75	0.092	34.02
Gas Flow Rate	3	2.30	2.30	0.77	1.02	0.494	6.02
Arc Gap	3	1.47	1.47	0.49	0.65	0.633	3.85
Error	3	2.26	2.26	0.75			5.91
Total	15	37.056					100

R-Sq = 94.1%   R-Sq(adj) = 70.4%

In ATIG welding of duplex steel 2205 with and without of nitrogen as a shielding gas, the current and welding speed plays a major role in deciding the depth of the penetration of the weld. The contribution of the levels of arc gap is not predominant in affecting the responses considered. The corresponding regression equations are:

$$\text{ATIG - Depth of penetration (mm)} = 1.67 + 0.0512\ C - 0.0600\ WS - 0.0353\ GFL - 0.363 AG \quad (3)$$

$$\text{ATIG+N-Depth of penetration (mm)} = 0.28 + 0.0526\ C - 0.0433\ WS - 0.0259\ GFL - 0.542 AG \quad (4)$$

With C: Current, WS: Welding speed, GFL: Gas flow rate and AG: Air gap.

EFFECTS OF PROCESS PARAMETERS:

The effects of the process parameters of Activated TIG welding on welding duplex stainless steel Using Argon and Argon + Nitrogen as shielding gas is obtained by plotting the main effects of the process parameters to the response considered are shown in response Tables 7 & 8 and plotted as response graphs in Figure 1 and 2 respectively.

Tab. 7 – Response table S/N ratio for depth of penetration ATIG (larger the better)

Process	Symbols	A	B	C	D
	Levels	**Current**	**Welding Speed**	**Gas Flow Rate**	**Arc Gap**
ATIG	1	12.25	15.32	13.16	13.65
	2	13.59	14.31	14.31	13.74
	3	14.08	13.21	14.13	13.68
	4	15.08	12.15	13.40	13.93

The optimum setting is A4B1C2D4

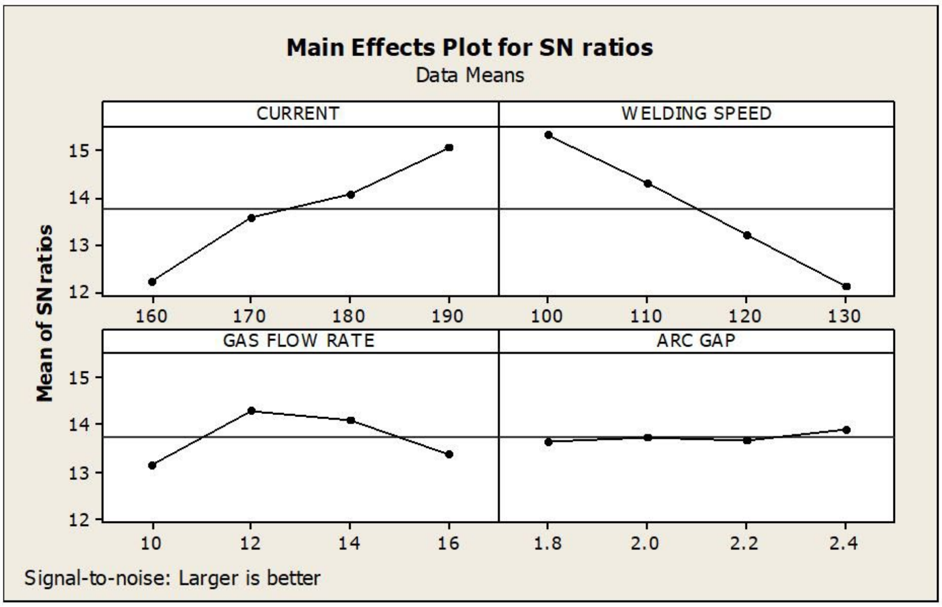

Fig. 1 – Main effects of S/N ratio for ATIG welds – depth of penetration

Tab. 8 – Response table S/N ratio for depth of penetration ATIG+N (larger the better)

Process	Symbols	A	B	C	D
	Levels	**Current**	**Welding Speed**	**Gas Flow Rate**	**Arc Gap**
ATIG	1	12.41	14.7	13.35	12.94
	2	12.64	13.7	13.95	13.65
	3	13.63	13.29	13.65	13.63
	4	15.19	12.18	12.92	13.65

The optimum setting is A4B1C2D4

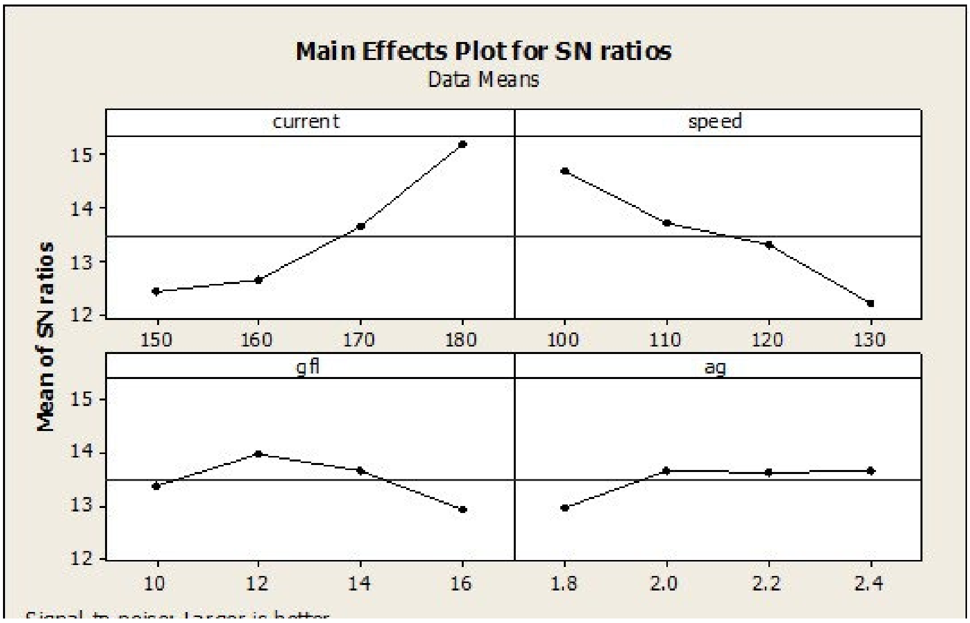

Fig. 2 – Main effects of S/N ratio for ATIG+N welds – depth of penetration

CURRENT

The welding current directly influences the heat input to the weld. Higher currents result in more heat input, which can improve penetration and fusion but can also cause excessive heat-affected zones (HAZ). Duplex stainless steels require a balanced microstructure of ferrite and austenite. High current levels can increase heat input, which promotes grain growth and may increase ferrite content. This can upset the balance, resulting in a greater amount of ferrite. Optimal current levels are required to preserve phase stability and prevent the production of undesired phases such as sigma or chi phases, which can be caused by excessive heat input and prolonged high-temperature exposure. The ideal current for ATIG welding duplex stainless steels should be determined by the material's thickness, joint configuration, and required weld qualities. It is typically necessary to fine-tune to get the optimal mix of penetration, microstructure control, and overall weld quality.

The current is the heat source of the process exhibits a linear relationship with the depth of the penetration and the area of the weld. The depth of penetration as well as the area of the weld increases with increase in the welding current is clearly visualized from both statistically as well as the weld macrostructure. The minimization of the aspect ratio is also achieved in increasing the welding current. The desired level of current in achieving maximum penetration and minimum aspect ratio is level 4 ie., 180 Amps for ATIG and ATIG+N.

WELDING SPEED

Welding speed effects cooling rate; greater speeds generally increase cooling rate, resulting in a larger ferrite content. Slower speeds, on the other hand, allow for greater time at higher temperatures, which promotes the development of austenite.

Proper welding speed contributes to the mechanical integrity of duplex stainless steel. High welding speeds may result in a higher ferrite content, increasing strength but decreasing toughness. Slow speeds might cause excessive austenite, weakening strength.Faster welding speeds typically produce narrower and shallower weld beads, which may not be sufficient for complete penetration welds in thicker materials. Slower speeds can improve penetration but may result in broader beads and an increased risk of overheating.

Excessive welding speeds might compromise weld pool stability, potentially resulting in porosity and incomplete fusion defects. In contrast, extremely slow rates can result in excessive heat input, creating weld metal dilution and increasing the danger of hot cracking. The ideal welding speed for duplex stainless steels must be carefully selected depending on the material thickness, welding technique, and desired weld qualities.

The function of the welding speed is to concentrate the heat source to a particular point. In order to maximize the depth of penetration and the area of the welds, the welding speed should be low as possible. The welding speed exhibits an inverse function with respect to the depth of penetration concerned. And it is clearly captured from the experiments. The minimization of the aspect ratio is also achieved in decreasing the welding speed. Thus, the welding speed at level 1 is the desired level for the responses considered i.e., the welding speed is to be set at100 mm/min for ATIG welding of duplex steel.

GAS FLOW RATE

The gas flow rate is one of the significant factors in ATIG welding process. The gas rate should not be low or so high, but a moderate gas flow rate is essential in determining the weld geometry and depth of penetration. The desired rate of gas flow is at second level for the responses considered i.e., the gas flow rate is to be set at 12 lit/min for ATIG welding of duplex steel.

ARC GAP

The air gap is one of the important factors in ATIG welding process. In our investigation the air gap doesn't affect the responses significantly. It should be inferred that within the selected range of process window it can be fixed at any level to get a desired output.

EFFECT OF NITROGEN

Nitrogen is essential in ATIG welding duplex stainless steels because it stabilises the austenite phase, increases corrosion resistance, improves mechanical characteristics, reduces porosity, and controls the heat-affected zone. Proper nitrogen level management is critical for producing high-quality welds with the necessary characteristics. Insufficient nitrogen can result in increased ferrite content, whilst too much nitrogen can induce porosity and other weld defects. The penetration of the weldments were reduced and controlled by the presence of nitrogen in the shielding gas mixture as well as the its governs the bead geometry of the welds by maintaining a good aspect ratio of the weld.

MACROSTRUCTURE

Macro structures of all the ATIG and ATIG+N welds (16 welds each) are shown in Figure 3 & 4. The macrostructure study shows the effect of various welding parameters on depth of penetration. It can be noticed from these macrographs that for ATIG and ATIG+N welds even small variations in current (Amps) and welding speed (mm/min) can affect the depth of penetration significantly and also points out the head of optimization of process parameter in order to achieve full penetration welds.

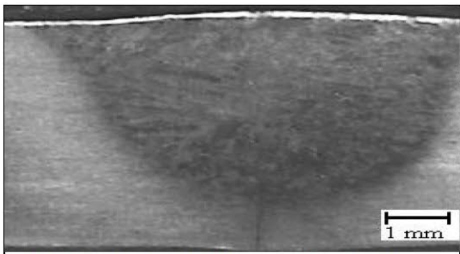

ATIGL1 D:4.78mm; W:6.94mm; W/D:1.45

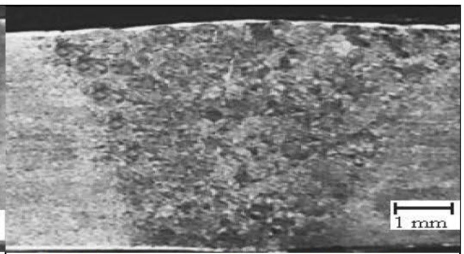

ATIGL5 D:6.12mm; W:7.47mm; W/D:1.22

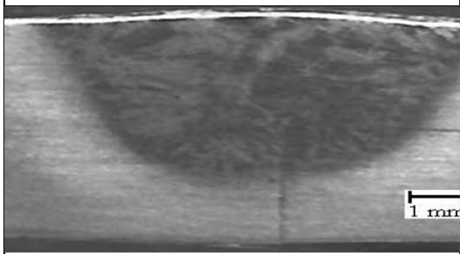

ATIGL2 D:4.56mm; W:7.29mm; W/D:1.59

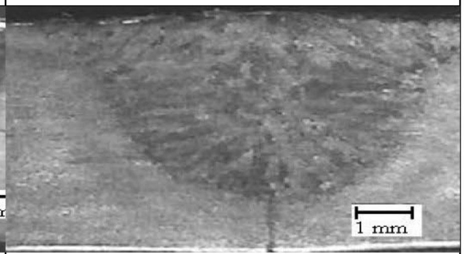

ATIGL6 D:4.67mm; W:7.72mm; W/D:1.65

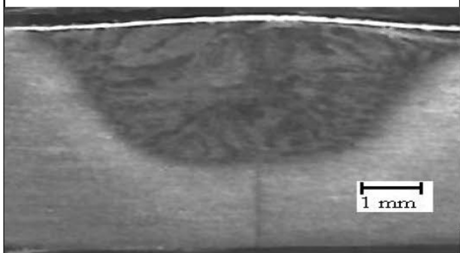

ATIGL3 D:3.83mm; W:7.34mm; W/D:1.91

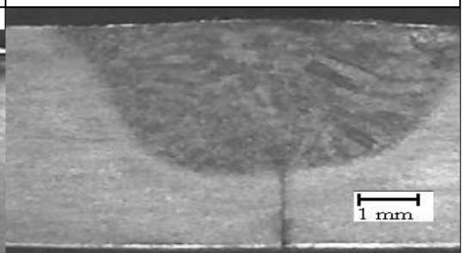

ATIGL7 D:4.18mm; W:7.26mm; W/D:1.73

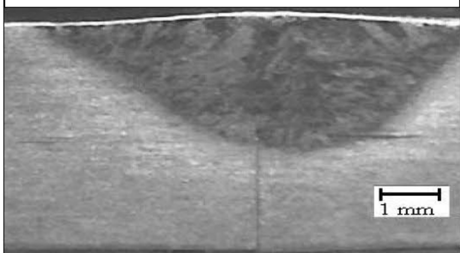

ATIGL4 D:3.37mm; W:7.42mm; W/D:2.20

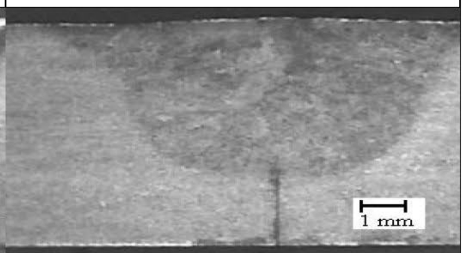

ATIGL8 D:4.37mm; W:7.15mm; W/D:1.63

Fig. 3 – Macrostructures of Bead Geometry (ATIGL1 – ATIGL8)

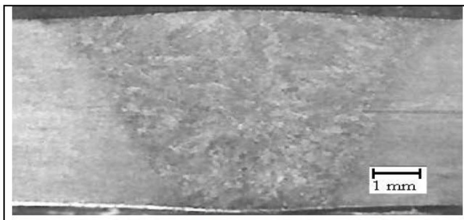 ATIGL9 D:6.34mm; W:8.33mm; W/D:1.31	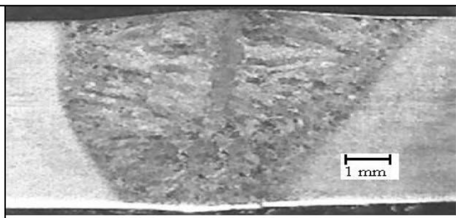 ATIGL13 D:6.26mm; W:7.96mm; W/D:1.27
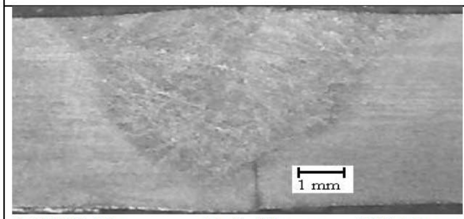 ATIGL10 D:5.42mm; W:7.9mm; W/D:1.45	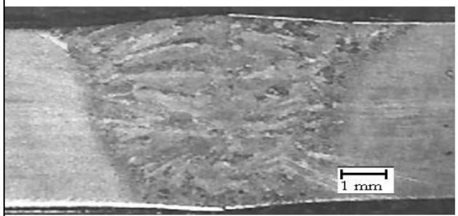 ATIGL14 D:6.31mm; W:7.72mm; W/D:1.22
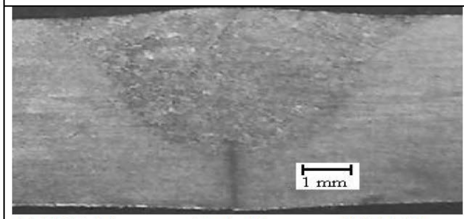 ATIGL11 D:4.48mm; W:7.23mm; W/D:1.61	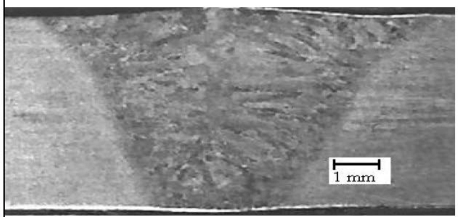 ATIGL15 D:6.12mm; W:8.28mm; W/D:1.35
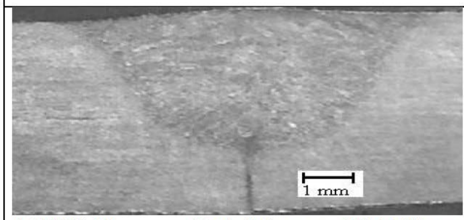 ATIGL12 D:4.26mm; W:7.05mm; W/D:1.65	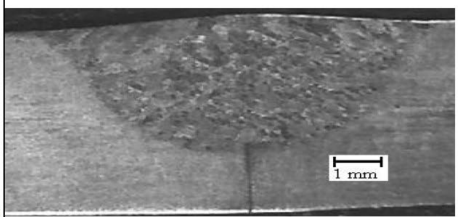 ATIGL16 D:4.29mm; W:7.91mm; W/D:1.84

Fig. 4 – Macrostructures of Bead Geometry (ATIGL9 – ATIGL16)

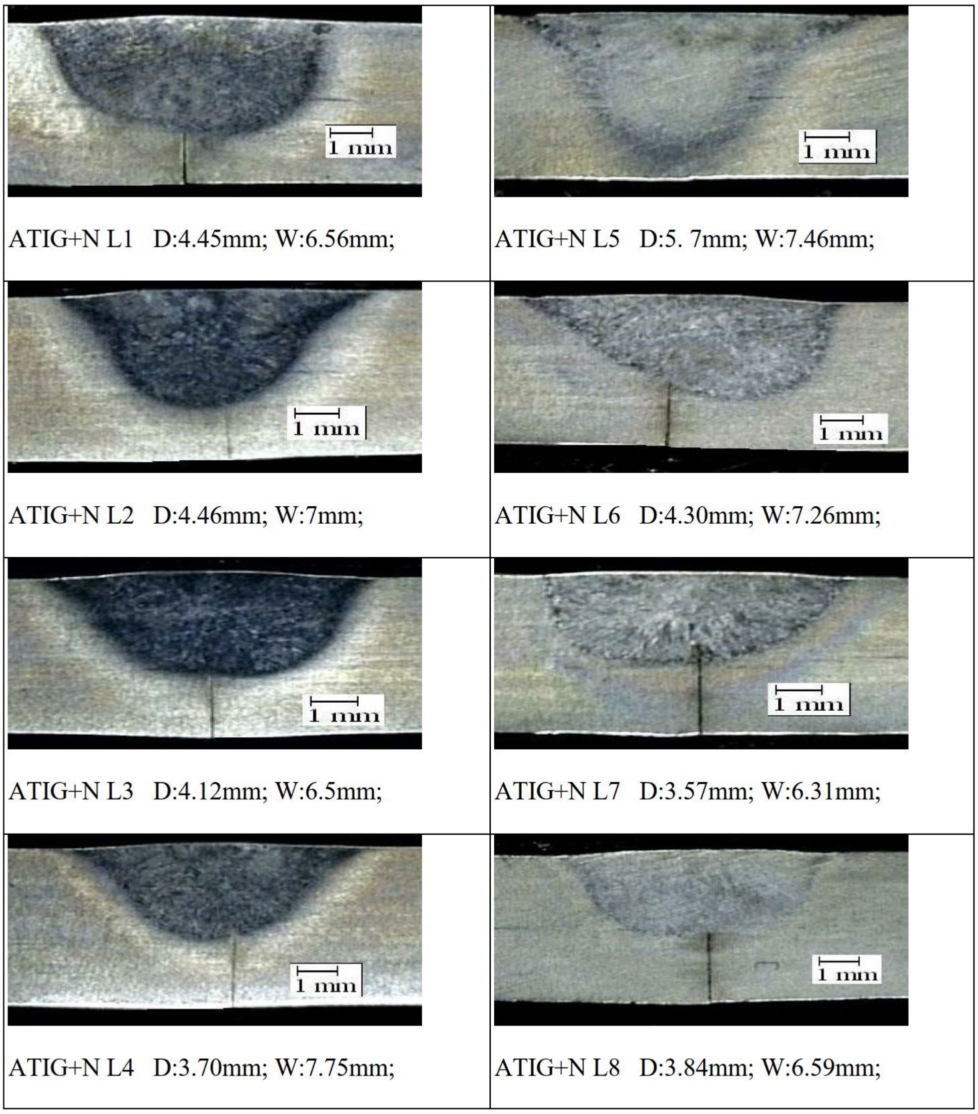

Fig. 5 – Macrostructures of Bead Geometry ATIG+N L1 – ATIG+N L8)

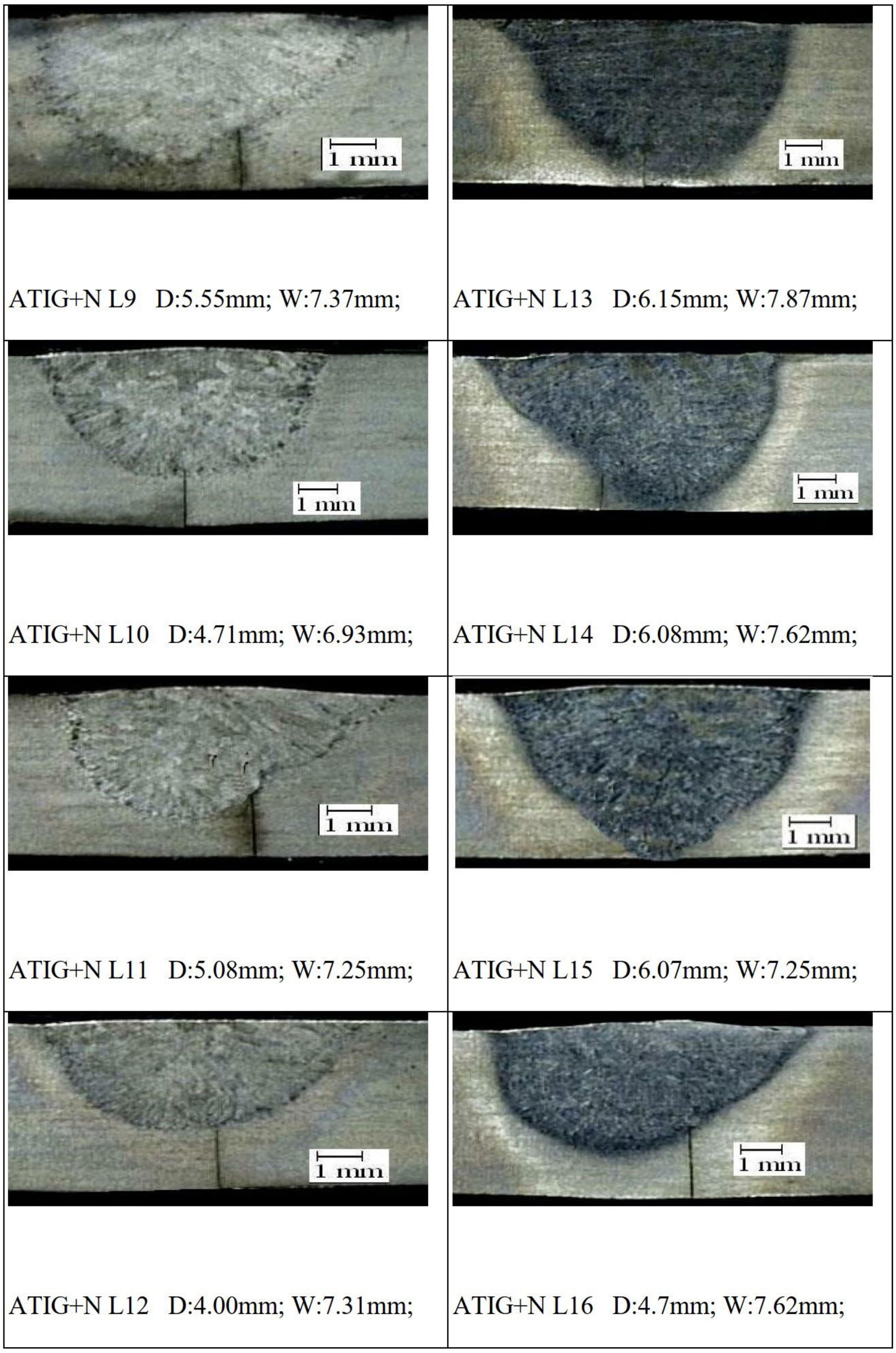

Fig. 6 – Macrostructures of Bead Geometry (ATIG+N L9– ATIG+N L16)

MICROSTRUCTURE

Duplex stainless steel (DSS) contains approximately equal proportions of body centered cubic ferrite (α) and face-centered cubic austenite (γ). Austenite stabilizers, such as nickel and nitrogen, promote the formation of austenite (γ phase), while ferrite stabilizers, such as chromium and molybdenum, promote formation of ferrite (α phase) respectively[17].The DSS base material microstructure and sem image is shown in Figure 5 ac & b which has Ferrite-Austenite dual phase banded structure. During welding the weld pool solidifies as ferrite, which on further cooling partially transforms to austenite.

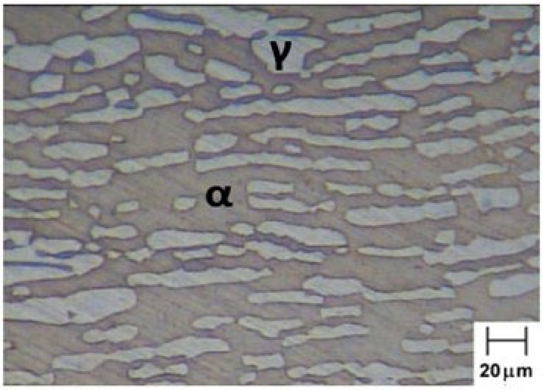

(a)

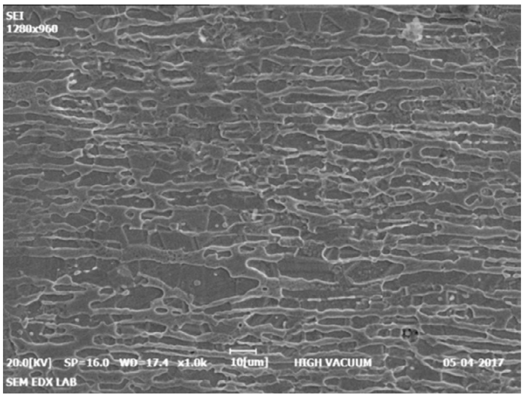

(b)

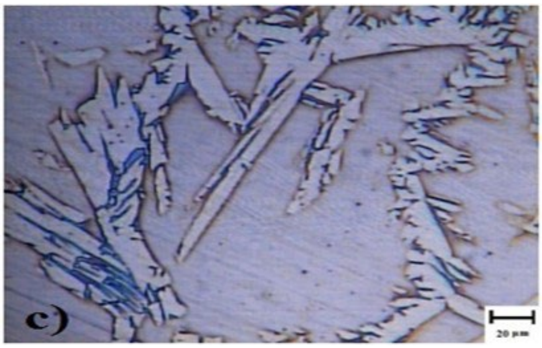

(c)

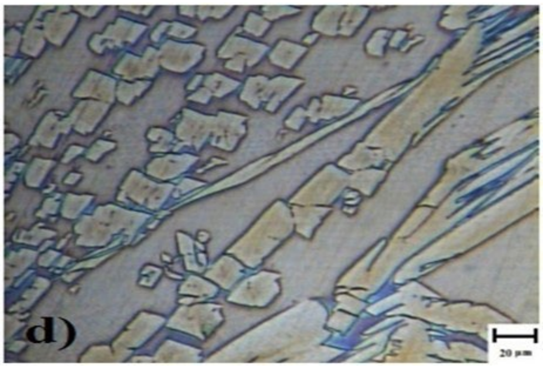

(d)

Fig. 7 – Microstructures of base material and welded joints: (a) Optical microstructure; (b) SEM micrograph; (c) ATIG;(d) ATIG + N

In Figure 5 c and d shows the microstructure of ATIG and ATIG +N welds. The ferrite content in the different weld zones were ATIG – 63% and ATIG+N – 55% whereas 54% ferrite is observed in the Base Metal is shown in table 9.

All duplex stainless steel weld metals solidify primarily as ferrite and, in the subsequent solid-state transformation, part of the ferrite transforms to austenite[7-9]F. This ferrite-to-austenite transformation takes place over a range of temperatures starting at the solvus temperature. However, the transformation cannot attain equilibrium on account of the rapid cooling, so that more ferrite remains untransformed than under equilibrium conditions. The transformation of ferrite to austenite during the welding of duplex stainless steel is similar to that in low carbon-steel weld metals where austenite transforms to ferrite on cooling. In low-carbon steels, first the proeutectoid ferrite forms at the prior-austenite grain boundaries; then the Widmanstätten side-plates nucleate at the grain boundaries and grow inward; and finally, the intragranular acicular ferrite forms in the regions partitioned by the side-plates.

In the case of a higher Nitrogen content welds like AuTIGN and AuATIGN, the areas of ferrite phases were surrounded by Austenite phase in large amounts. The weld specimens show only dual phase structure of α ferrite and γ austenite [10,12-15]. Weld metals which experience Faster cooling rates result in higher ferrite and lower austenite compared to parent material. Figure 5 c and d shows the microstructure of ATIG and ATIG +N welds. The ferrite content in the different weld zones were ATIG – 63% and ATIG+N – 55% whereas 54% ferrite is observed in the Base Metal is shown in table 9.

Tab. 9 – % of Ferrite of Duplex Stainless Steel weld metal (confirmation run) - Base Metal, ATIG & ATIG+N

S.No	Specimen Designation	% Ferrite
1	BM	54
2	ATIG	63
3	ATIG+N	55

OPTIMUM LEVEL OF PROCESS PARAMETER

The effects of the process parameters of ATIG welding on welding duplex stainless steel is clearly shown by plotting the main effects of the process parameters to the concern response considered. And it is summarized below for each process parameter. Based on the L16 experiments, the optimum level settings for depth and aspect ratio are A4B1C2D4 and A4B1C2D4respectively.)The average values of the factors at their levels are taken from the Table 5 and the predicted value of the response is given in the table 10 [12 &24].

ATIG :

Depth of Penetration (predicted)

$$=A4+B1+C2+D4-3T \quad (5)$$
$$=5.745+5.875+5.265+5.125-3(4.96)$$
$$=7.13 \text{ mm}$$

where

A 4 : Average mean value of Current at 4th level.

B 1 : Average mean value of Welding speed at 1st level.

C 2 : Average mean value of Gas flow rate at 2nd level.

D 4 : Average mean value of Arc gap at 4th level.

T : Overall Mean (Depth of Penetration)

ATIG+N :

Depth of Penetration (predicted)

$$=A4+B1+C2+D4-3T \quad (6)$$
$$=5.42+4.53+4.90+4.91-3(4.57)$$
$$=6.05 \text{ mm}$$

where

A 4 : Average mean value of Current at 4th level.

B 1 : Average mean value of Welding speed at 1st level.

C 2 : Average mean value of Gas flow rate at 2nd level.

D 4 : Average mean value of Arc gap at 4th level.

T : Overall Mean (Depth of Penetration)

Tab. 10 – Predicted optimal levels for confirmation run (ATIG & ATIG+N)

S.No.	Responses		Optimal parameter
1	Depth of penetration	ATIG	A4B1C2D4
2		ATIG+N	A4B1C2D4

CONFIRMATION RUN

The confirmation experiments were carried out by setting the process parameters at optimum levels for different responses considered. At the optimum settings full penetration of the welds is achieved and the values obtained in the confirmation run are shown in Table 11. The macrostructures of the confirmation runs are shown in Figure 6.

Tab. 11 – Predicted and confirmation run values for ATIG & ATIG+N

S.No.	Response	Predicted	Optimal parameter
1	Depth of penetration	7.13 mm	A4B1C2D4
2		6.05 mm	A4B1C2D4

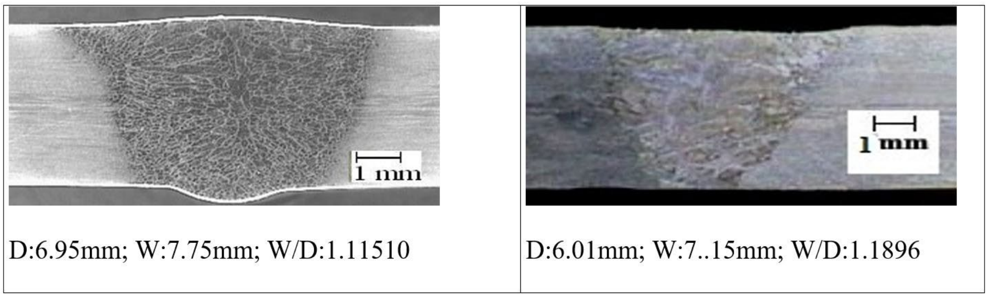

Fig.8 – a) Macrostructure of bead geometry for confirmation run (DOP) ATIG: b) Macrostructure of bead geometry for confirmation run (DOP) ATIG+N

CONCLUSIONS

The Activated flux significantly increases the Depth of penetration for a given current value for full penetration, 180 A was found to be sufficient against 250A required for welding DSS plates without flux.

It has been found that Autogenous ATIG welding with Argon + 2% Nitrogen as shielding gas can be used to produce sound welds on 6mm thick 2205 DSS plates in single pass.

Current and Welding Speed plays a vital role in heat input of the process and is highly significant in influencing the Depth of penetration of the weld. As well as both the parameters are highly significant in affecting aspect ratio of the welds in both ATIG and argon, nitrogen mixture ATIG welding.

The presence of nitrogen in the shielding gas mixture lowers and controls the weld penetration while also governing the bead shape of the welds by keeping a proper aspect ratio.

ACKNOWLEDGEMENT

The authors thankfully acknowledge the financial support for this research provided by All India Council for Technical Education (AICTE) – Research Promotion Scheme (RPS), Government of India, under the Grant No. AICTE/RIFD/RPS(POLICY-III)32/2012-13.

REFERENCES

[1] Chern, TS, Tseng, KH & Tsai, HL 2011, 'Study of the characteristics of duplex stainless steel activated tungsten inert gas welds', Materials and Design, vol. 32, pp. 255-263 DOI:10.1016/j.matdes.2010.05.056

[2] Chuan-Ming Tseng 2003, 'The influence of nitrogen content on corrosion fatigue crack growth behavior of duplex stainless steel', Materials Science and Engineering, vol. A 344, pp.190-200.

[3] Fisher, RA 1925, 'Statistical methods for research worker', Olive and Boyd, London, UK.

[4] Fujii, H , Sato, T, Lu, S P, Nogi, K, 'Development of an advanced A-TIG AA-TIG, welding method by control of Marangoni convection', Materials Science and Engineering A 495 2008, pp. 296-303 DOI:10.1016/j.msea.2007.10.116

[5] Huang, HY, Shyu, SW, Tseng, KH & Chou, CP 2005, 'Evaluation of TIG flux welding on the characteristics of stainless steel', Science and Technology of Welding and Joining, vol. 10, no. 5, pp. 566-573 DOI:10.1179/174329305X48329

[6] Huang, HY, Shyu, SW, Tseng, KH & Chou, CP 2006, 'Effects of the process parameters on austenitic stainless steel by TIG-flux welding', Journal of Materials Science & Technology, vol. 223, pp. 367-374

[7] Huang, L, Deng, X, Liu, J& Wang, Z 2016, 'Relationship Between Retained Austenite Stability and Cryogenic Impact Toughness in 0.12 C-3.0 Mn Low Carbon Medium Manganese Steel', Acta Metall. Sin., vol. 53, pp. 316-324.

[8] Iris Alvarez-Armas 2008, 'Duplex stainless steels: brief history and some recent alloys', Recent Patents on Mechanical Engineering, vol. 1, pp. 51–57.

[9] Karlsson, L 1994a, 'Welding duplex and super duplex stainless steels', Svetsaren, vol. 48, no. 2, pp. 5-10.

[10] Karlsson, L 1994b,' Welding of modern duplex stainless steels', Proceedings of the Pre-assembly Symposium on Welding, Joining, Coating and Surface Modification of Advanced Materials, Dalian, China, pp. 49-60.

[11] Koil Raj, M, Vijayan, S & Rao, SRK 2012, 'Friction stir welding of dissimilar aluminum alloys: AA2219 to AA5083 – Optimization of process parameters using Taguchi method', Materials and Design, vol. 42, pp. 1-7 DOI:10.1016/j.matdes.2012.02.016

[12] Kokawa, H, Kuwana, T & Okada, J 1993, 'Nitrogen absorption and microstructure of duplex stainless steel weld metal', Welding International, vol. 7, no. 5, pp. 384-389.

[13] Kokawa, H, Okada, J & Kuwana, T 1992, 'Nitrogen absorption and microstructure of duplex stainless steel weld metal', Q Journal of Japan Welding Society, vol. 10, no. 4, pp. 496-502.

[14] Kokawa, H, Okada, J & Kuwana, T 1993, 'Effect of nitrogen on tensile properties of duplex stainless steel weld metal', Q Journal of Japan Welding Society, vol. 11, no. 4, pp. 531-53.

[15] Kokawa, H, Yomito, M, Kuwana, T 1995, 'Effect of nitrogen on impact toughness of duplex stainless steel weld metal', Welding International, vol. 9, no. 3, pp. 8-14.

[16] Lu, SP, Li, DZ, Fujii, H & Nogi, K 2007, 'Time dependant weld shape in Ar-O2 shielded stationary GTA welding', Journal of Materials Science and Technology, vol. 23, no. 5, pp. 650-654.

[17] Nilson, JO 1992, 'Overview- super duplex stainless steels', Materials Science and Technology, 8.8, 685-700.

[18] Ogawa, T, Aoki, S, Sakomoto, R &Zaizen, T 1982, 'The weldability of nitrogen-containing austenitic stainless steel: Part 1 – chloride pitting corrosion resistance', Welding Journal, vol. 61, no. 5, pp. 139-148.

[19] Okagawa, RK, Dixon, RD, Olson DL 1983, 'The influence of nitrogen from welding on stainless steel weldmetal microstructures', Weld journal, vol. 62, pp.204-208.

[20] Sathiya, P, Aravindan, S & Noorul Haq, A 2006, 'Optimization for friction welding parameters with multiple performance characteristics', International Journal of Mechanical Material Design, vol. 3, pp. 309-318, DOI:10.1007/s10999-007-9037-z

[21] Stephenson, N 1987, 'Welding status of duplex stainless steels for offshore Applications', Part I. Welding & Metal Fabrication, pp. 159-164.

[22] Still, JR 1994a, 'The use of duplex Stainless steel in the offshore and oil and gas industry – Part I', Welding & Metal Fabrication, pp. 293-296.

[23] Still, JR 1994b, 'The use of duplex Stainless steel in the offshore and oil and gas industry – Part II', Welding & Metal Fabrication, p. 331-339.

[24] Sasidharan, R, Rajendra Boopathy, S, Vijayan, S & Koteswara Rao, SR 2016, 'Optimization of bead geometry for duplex stainless steel GTA welds using the Taguchi approach', Materials Testing, vol. 58, no. 4, pp. 312-318, DOI 10.3139/120.110854.

[25] Puren Liu, Ming Liu, Qing Zheng, Lining Xu, Lijie Qiao, Yu Yan,"Study on the failure mechanism of the heat-affected zone in 2205 duplex stainless steel weld-joints induced by hydrogen,"Corrosion Science,Volume 244,2025,112657,ISSN 0010-938X,https://doi.org/10.1016/j.corsci.2024.112657.

[26] Flávia Wagner Pinheiro, Lucas Menezes de Souza, Elaine Cristina Pereira, Sergio N. Monteiro, Afonso R.G. Azevedo, "Effect of solubilization heat treatment on microstructure and corrosion resistance of joints welded with the autogenous TIG process duplex stainless steel," Journal of Materials Research and Technology," Volume 26,2023, Pages 1527-1536, ISSN 2238-7854.https://doi.org/10.1016/j.jmrt.2023.08.014

[27] Guangnan Ge, Shawei Tang, Jin Hu, Yan Huo, Caimeng Qi, Kuiliang Zhang, Yi Liu, Jing Li,Influence of arc energy on the microstructure and corrosion behavior of ER2209 duplex stainless steel deposited on Q345B low-alloy steel by GMAW,Materials Today Communications,Volume 41,2024, 110778,ISSN 2352-4928, https://doi.org/10.1016/j.mtcomm.2024.110778.

[28] Kanglong Wu, Chen Shen, Peizhi Xu, Jianwen Xin, Yuhan Ding, Lin Wang, Wenlu Zhou, Gang Ruan, Yuelong Zhang, Fang Li, Man-Tai Chen, Xueming Hua,Revealing the evolution of microstructure and mechanical properties with deposition energy and shielding gas

to achieve phase-balanced directed energy deposition of 2205 duplex stainless steel,Materials Science and Engineering: A, Volume 915,2024,147197,ISSN 0921-5093,https://doi.org/10.1016/j.msea.2024.147197.

[29] Qi Wang, Guochao Gu, Chuanbao Jia, Kan Li, Chuansong Wu,Investigation of microstructure evolution, mechanical and corrosion properties of SAF 2507 super duplex stainless steel joints by keyhole plasma arc welding, Journal of Materials Research and Technology, Volume22, 2023, Pages355- 374,ISSN22387854,https://doi.org/10.1016/j.jmrt.2022.11.107.

TORNA ALL'INDICE >